Liu et al. Protection and Control of Modern Power Systems (2017) 2:39
DOI 10.1186/s41601-017-0070-0

Protection and Control of Modern Power Systems

ORIGINAL RESEARCH Open Access

PV-based virtual synchronous generator with variable inertia to enhance power system transient stability utilizing the energy storage system

Ju Liu[1*], Dongjun Yang[1], Wei Yao[2], Rengcun Fang[1], Hongsheng Zhao[1] and Bo Wang[1]

Abstract

The Photovoltaic (PV) plants are significantly different from the conventional synchronous generators in terms of physical and electrical characteristics, as it connects to the power grid through the voltage-source converters. High penetration PV in power system will bring several critical challenges to the safe operation of power grid including transient stability. To address this problem, the paper proposes a control strategy to help the PVs work like a synchronous generator with variable inertia by energy storage system (ESS). First, the overall control strategy of the PV-based virtual synchronous generator (PV-VSG) is illustrated. Then the control strategies for the variable inertia of the PV-VSG are designed to attenuate the transient energy of the power system after the fault. Simulation results of a simple power system show that the PV-VSG could utilize the energy preserved in the ESS to balance the transient energy variation of power grid after fault and improve the transient stability of the power system.

Keywords: Energy storage system, Virtual synchronous generator, Variable inertia, Transient stability, Photovoltaic power

1 Introduction

Photovoltaic (PV) power is one of the prominent renewable resources and likely to replace a significant proportion of fossil-fuels in the future. With the increasing penetration of PV power, power system operators will encounter severer challenges [1–3]. Unlike synchronous generators, PVs are connected to the power grid through the voltage-source converters (VSCs). Thus, the PVs are significantly different from the conventional synchronous generators in terms of physical and electrical characteristics. Thus the high penetration PVs will deteriorate the frequency stability of power system. For the protection of the PVs, the power system with high penetration PVs must own the capacity of low voltage and high voltage ride through. What is more, the transient stability of power system with high penetration PVs is also a problem should be followed.

Transient stability is the ability of the power system to maintain synchronism when subjected to a severe disturbance such as a fault on transmission facilities, loss of generation, or loss of a large load. In the case of disturbances, conventional synchronous generators (SGs) are able to utilize the kinetic energy preserved in their rotational inertia to balance the potential energy variation of the power grid. Therefore, the system tends to stabilize again after disturbances. However, the inverter-based photovoltaic (PV) power stations do not have rotating elements and usually operate under the maximum power point tracking (MPPT) control strategy, which means it could not provide adequate energy, neither kinetic energy nor potential energy, to stabilize the power grid. Consequently, a power system with high-penetration of PV is prone to lose stability once disturbed.

In recent years, as an important part of smart grid, energy storage system (ESS) has been widely applied in power system [4–6]. One of the applications is the virtual synchronous generator. The VSG control strategy of ESS has been introduced as a promising solution to

* Correspondence: liujuhust@qq.com
[1]State Grid Hubei Economic Research Institute, Wuhan, China
Full list of author information is available at the end of the article

improve the stability characteristic of power system with high penetration renewable power. The VSG systems addressed in [7–9] are designed to connect an energy storage unit to the main grid. Rather than the traditional phase locked loop (PLL), the VSGs utilize the swing equation to synchronize with the grid. The VSGs could provide better active and reactive power to the power grid to improve the stability of power grid [10, 11]. In [12–15], different virtual synchronous generator control strategies have been proposed to improve the frequency, voltage, transient stability and damping characteristic of power system with renewable power generators. In [16, 17], the control strategies are designed to control the PVs and wind power to emulate the behaviors of the synchronous generators with energy storage system.

VSGs could model the rotational inertia of a synchronous generator through coordinating the active power output of the PV power station and an energy storage system (ESS) [18]. Once disturbed, the electrical power stored in the ESS could be exploited to dissipate the unbalanced energy. Then the power system with high penetration PVs could recover to a stable state. Moreover, the virtual moment of inertia of the VSG is adjustable, which is more beneficial to the transient stability of the power system than the fixed moment of inertia of SGs. Hence, this paper explores the feasibility of improving the transient stability of power system by using PV-VSG control strategy with variable inertia.

Different to the PV-VSG for frequency stability improvement, the main purpose of our research is to improve the transient stability of the power system. Thus the control strategy of the virtual inertia of the PV-VSG is also different from that of the PV-VSG for frequency stability improvement. In our paper, the PV-VSG control strategy is adopted to improve the transient stability of the power system. In order to achieve this goal, the virtual inertia of the PV-VSG should change according to the change of the transient energy of the power system. Hence, the main innovation and contribution of this paper is that a variable inertia control strategy of the PV -ESS is purposed according to the change of the transient energy of the power system, which is different from the PV-VSG for frequency stability improvement.

The rest of the paper is organized as follows. The overall PV-VSG control strategy is described in section 2. Section 3 proposes the inertia control strategy for transient stability improvement of power system with PV-VSG. A case study is undertaken on power system to verify the effectiveness of the proposed strategy in section 4. Discussion and Conclusions are drawn in section 5 and 6 respectively.

2 PV-VSG control strategies

VSC based converters have no inertia and the frequency of them is controlled just to follow grid frequency. Thus power systems will become unstable with high penetration PVs. Since synchronous generators have good capacity to regulate the frequency of power system, the concept that converters are controlled to express as a synchronous generator has been proposed which is called VSG. In this paper, we propose the PV-VSG control strategy to control the power output of the VSC based PVs and the ESS. The overall control strategy of the PV-VSG will be introduced in the follows.

2.1 Overall control scheme

Figure 1 shows the overall control scheme of the PV-VSG control strategy. The PV power station and the ESS are connected to the same point of common coupling (PCC) through step-up transformers. For convenience, the PV-ESS combined system will from now on be referred to as "PV-VSG". Since the PV power station is operating under the MPPT control strategy, the active power output of the PVs totally depends on the real-time solar radiation intensity and temperature. The active power output of the ESS is determined by the PV-VSG control strategy. The PV-VSG controller measures the voltage V_{grid} and the current I_{grid} at the PCC bus to calculate the power output P_{out} of the PV-VSG and the rotation speed ω_{grid} of the power grid. Then the PV-VSG controller gives out the rotation speed deviation $\Delta\omega_{\text{VSG}}$ of the PV-VSG and the ESS controller calculate the reference power output of the ESS. The detail control strategy of the controllers will be given out in the fellows.

2.2 Block diagram of VSG control strategy

The detailed control strategy block diagram of the PV-VSG controller is shown in Fig. 2. The PV-VSG control strategy aims at modeling the well-known swing equation of SGs:

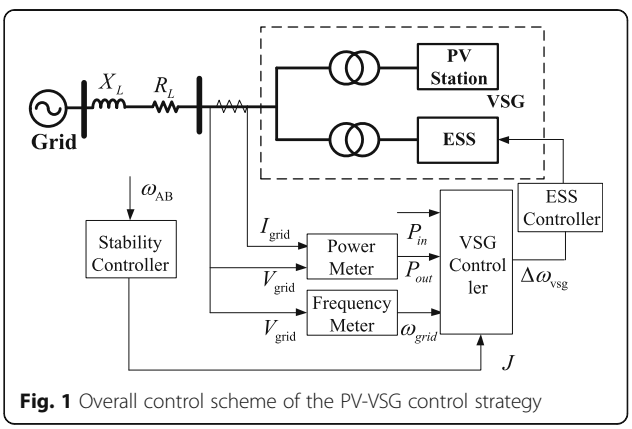

Fig. 1 Overall control scheme of the PV-VSG control strategy

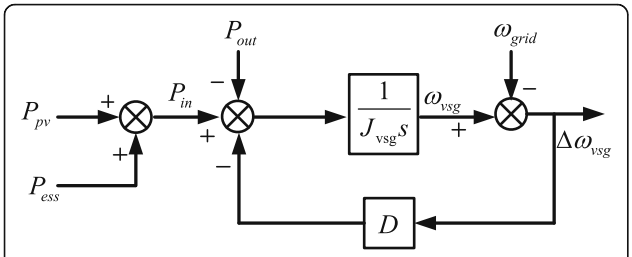

Fig. 2 Block diagram of VSG control strategy

$$J_{\mathrm{vsg}}\frac{d\omega}{dt} = P_{in} - P_{out} - D\left(\omega_{vsg} - \omega_{grid}\right) \quad (1)$$

where P_{in}, P_{out}, J_{vsg}, ω_{vsg} and D are the input power (the same as the prime mechanical power of the SG), the output power, the virtual moment of inertia, the virtual angular velocity, and the virtual damping factor of the VSG, respectively. ω_{grid} is the grid frequency, P_{pv} and P_{ess} is the power output of the PVs and the ESS. The input power P_{in} of the VSG controller is the total power injected to the power grid by the PVs and the ESS.

2.3 Block diagram of ESS control strategy

Figure 3 illustrates the control block diagram of the ESS. In this model, the state of charge (SOC) level is ignored, since the transient process is within only several seconds. The dynamics of ESS is presented as a first order transfer function as follows:

$$P_{ess} = \Delta\omega_{vsg}\frac{K_{ess}}{T_{ess}s+1} \quad , \quad -P_{\max} \le P_{ess} \le P_{\max} \quad (2)$$

where K_{ess}, T_{ess}, P_{ess} and $P_{\max}$ are the gain, time constant, active power output and maximum power output of the ESS, respectively. If P_{bess} is positive, the ESS releases energy to the power grid, otherwise, it absorbs energy from the power grid.

Since the stability controller is the main contribution of this paper, the next section will show the main idea of the stability controller.

3 Methods

The main purpose of the stability controller is to give out a variable inertia of the PV-VSG, thus the transient energy of the power system will attenuate and the power grid with PVs will recover to a stable state after the disturbance. This section will analyze the transient energy of the power system after the fault and obtains the relation between the virtual inertia of the VSG and the transient energy. According to the above relation, the virtual inertia control strategy of the PV-VSG is designed to make the transient energy decay to zero after disturbance.

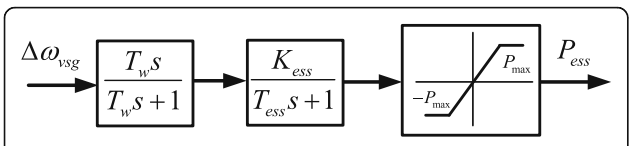

Fig. 3 Block diagram of ESS control strategy

3.1 Transient energy function (TEF)

A two-area power system is shown in Fig. 4. According to [2], the TEF can be used as a measurement of the unbalanced power when the power system is under disturbance. The transient energy (TE) of the power system is defined as follows:

$$\mathrm{TE} = \frac{1}{2}\omega_{AB}^2 - \int_{\delta_{AB0}}^{\delta_{AB}}\left[\frac{(P_{A0}-P_A)}{J_A} - \frac{(P_{B0}+P_B)}{J_B}\right]d\delta_{AB} \quad (3)$$

where δ_{AB} and ω_{AB} denote the difference in power angles and angular speed between the center of inertia (COI) of areas A and B, respectively. P_{A0} and $P_{B0}$are the intimal differences between the total power generation and consumption in the two areas. P_A and P_B are the transmission power as shown in Fig. 4. J_A and J_B denote the moment of inertia of the two areas.

In (3), the first and second terms are the transient kinetic energy (TKE) and the transient potential energy (TPE), respectively. When a fault occurs, the power system will oscillate correspondingly. The transient KE and transient PE will transform mutually, however, their sum, the total OTEF will remain constant for a zero-damped oscillation. Hence the TEF descent method can be proposed to design an inertia controller to dissipate the unbalanced energy and suppress the power oscillation. Thus the power system recoveries to a stable state after fault quickly.

3.2 TEF descent method

As shown in Fig. 5, the transmission power of the tie line will oscillate after a disturbance. For one cycle of the power oscillation, it could be divided into the following four phases.

Phase I is the backward acceleration phase. In this phase, the difference of the angular speedω_{AB} between the two areas is less than zero and the differential rate of ω_{AB} is also

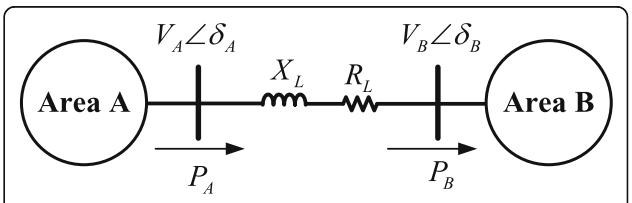

Fig. 4 Two area power system

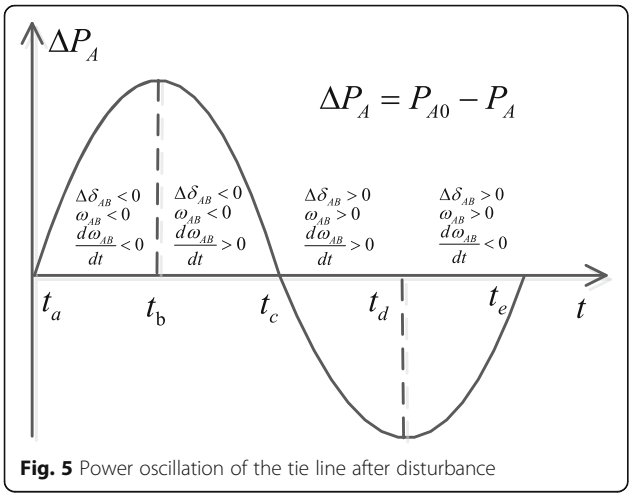

Fig. 5 Power oscillation of the tie line after disturbance

less than zero. As a result, ω_{AB} will decrease from zero to a minimum value $\omega_{AB\min}$ and δ_{AB} will also decrease. The transmission power of the tie line will decrease to the minimum value, and the power change of the transmission power ΔP_A will increase from zero to the maximum value as shown in Fig. 5 during the time from t_a to t_b.

Phase II is the backward deceleration phase. As shown in Fig. 5 during the time from t_b to t_c, $d\omega_{AB}/dt > 0$ and ω_{AB}will increase from the minimum value to zero. The difference of the angular speed satisfies $\omega_{AB\min} < \omega_{AB} < 0$.

Phase III is the forward acceleration phase. During the time from t_b to t_c, the differential rate of ω_{AB} keeps larger than zero. Thus the difference of the angular speed ω_{AB} between the two areas will across zero to be positive and will reach the maximum value. That means $0 < \omega_{AB} < \omega_{AB\max}$ and $d\omega_{AB}/dt > 0$.

Phase IV is the forward deceleration phase. In this phase, during the time $t \in [t_d, t_e]$ as shown in Fig. 5, $0 < \omega_{AB} < \omega_{AB\max}$ and $d\omega_{AB}/dt < 0$.

For the four phases, the TPE and the TKE will convict to each. If the damping of the power system is zero, the TEF of the power system will keep constant. After one cycle the TPE and the TKE will return to its initial state. The TPE at the time t_e could be calculated from the TPE at the time t_a by the following equation.

$$\mathrm{TPE}(t_e) = \mathrm{TPE}(t_a) - \int_{\delta_{AB(t_a)}}^{\delta_{AB(te)}} -\left[\frac{(P_{A0}-P_A)}{J_A} - \frac{(P_{B0}+P_B)}{J_B}\right] d\delta_{AB} \quad (4)$$

If we assuming that the damping of the power grid is zero, the TPE at the time t_a and t_e will equal to each other. That means$\mathrm{OPE}(t_e) = \mathrm{OPE}(t_a)$, and we could obtain:

$$\int_{\delta_{AB(t_a)}}^{\delta_{AB(te)}} \left[\frac{1}{J_A}(P_{A0}-P_A) - \frac{1}{J_B}(P_{B0}+P_B)\right] d\delta_{AB} = 0 \quad (5)$$

Form (5), it could be easily found that if the inertia of the two areas could be controlled, the TPE of the power system could decent after one cycle, also the decreasing of the TE will follow. Since the inertia of the VSG is adjustable unlike SG, a suitable variable inertia control strategy of the VSG could be adopted to improving the transient stability of the power system. In this paper, we assume that the VSG is on the receiving side area B. If we want to make the TPE attenuate during one oscillation cycle, the following strategy could be designed. In phases I and II, $(P_{B0}+P_B)d\delta_{AB} > 0$, let $\frac{1}{J_B} = \frac{1}{J_B} + \frac{1}{\Delta J}$; in phases III and IV, $(P_{B0}+P_B)d\delta_{AB} < 0$, let $\frac{1}{J_B} = \frac{1}{J_B} - \frac{1}{\Delta J}$. Then the OPE at the time t_e becomes:

$$\begin{aligned}\mathrm{OPE}(t_e) = \mathrm{OPE}(t_a) &+ \int_{\delta_{AB(t_a)}}^{\delta_{AB(tc)}} -\left[\frac{(P_{A0}-P_A)}{J_A} - \left(\frac{1}{J_B}+\frac{1}{\Delta J}\right)(P_{B0}+P_B)\right] d\delta_{AB} \\ &+ \int_{\delta_{AB(tc)}}^{\delta_{AB(te)}} -\left[\frac{(P_{A0}-P_A)}{J_A} - \left(\frac{1}{J_B}-\frac{1}{\Delta J}\right)(P_{B0}+P_B)\right] d\delta_{AB}\end{aligned} \quad (6)$$

Taking (5) into (6), the following equation could be gotten:

$$\mathrm{TPE}(t_e) = \mathrm{TPE}(t_a) - \Delta\mathrm{TPE} \quad (7)$$

where:

$$\begin{aligned}\Delta\mathrm{TPE} = &\int_{\delta_{AB(tc)}}^{\delta_{AB(ta)}} \left[\frac{1}{\Delta J}(P_{B0}+P_B)\right] d\delta_{AB} \\ &+ \int_{\delta_{AB(tc)}}^{\delta_{AB(te)}} \left[\frac{1}{\Delta J}(P_{B0}+P_B)\right] d\delta_{AB}\end{aligned} \quad (8)$$

Since during the time from $t_a$to t_c, $d\delta_{AB} < 0$ and $P_{B0} + P_B < 0$, the first term in (8) is larger than zero. The second term in (8) is also larger than zero because $d\delta_{AB}$ and $P_{B0} + P_B$ are both larger than zero during the time from t_c to t_e. Thus with the control strategy proposed above, ΔTPE will be a positive value. The total TEF will descend continuously in every oscillation cycle and hence the unbalanced energy will be efficiently dissipated and the power swing will be effectively suppressed. The transient

stability of the power system with high penetration PVs could be enhanced.

3.3 Stability controller for the VSG

From the TEF analysis in TEF descent method, it is easy to found that when the difference of the angular speed ω_{AB} between the two areas is large than zero, increasing the virtual inertia of the PV-VSG is beneficial for the stable of the power system. When $\omega_{AB} < 0$, decreasing the virtual inertia of the PV-VSG could improve the stability of the power system. According to this rule, a bang-bang control strategy of VSG's moment of inertia is proposed. The control strategy is illustrated in Fig. 6. J_{vsg} is the variable moment of inertia of the PV-VSG. It is consisted by the variable part ΔJ and constant part J_{con}. ΔJ is a positive value, ε is a small value chosen to eliminate measurement errors. Since in phase I and II, the difference of the angular speed ω_{AB} is large than zero, the inertia of the VSG will be increased by ΔJ. The inertia of the VSG will be decreased by ΔJ when $\omega_{AB} < 0$. By applying this control strategy, the transient energy of the PV power system will attenuate quickly after the disturbance. Thus the transient stability of the PV power system will be enhanced.

4 Results

4.1 Description of the test system

In this paper, a two-machine two-area test system is modeled on the platform of MATLAB/Simulink, as shown in Fig. 7. In this model, the synchronous generator (SG) is on the sending side, the VSG is on the receiving side. They are connected through an 110 kV double-circuit AC transmission line with constant-power loads. In the system, $S_B = 100\text{MW}$, $V_B = V_N$, $f_B = 50\text{Hz}$.

To verify the effectiveness of the proposed control strategy of VSG's moment of inertia, the following three typical control strategies are chosen to be studied.

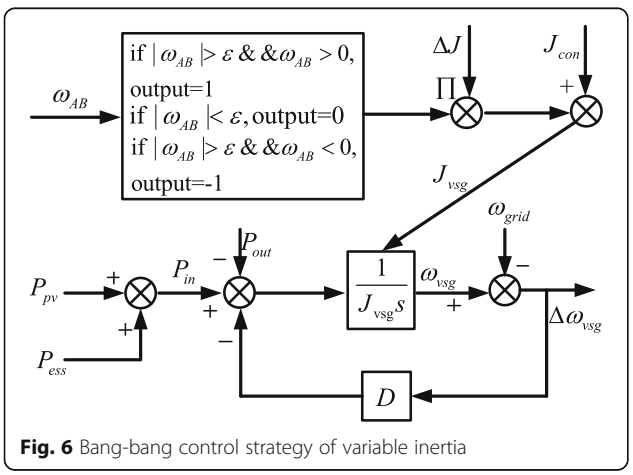

Fig. 6 Bang-bang control strategy of variable inertia

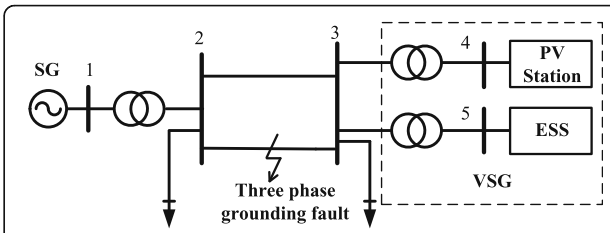

Fig. 7 Two-machine two-area system with PV-VSG integration

MPPT: No VSG control strategy is applied, and the PV is operated under the MPPT mode.

Variable inertia: PV-BESS combined system operates under the modified VSG control strategy, the virtual moment of inertia is controlled by the bang-bang control strategy.

Constant inertia: PV-BESS combined system operates under the traditional VSG control strategy, the virtual moment of inertia is fixed. It is chosen as the average value of the inertia under the bang-bang control strategy.

4.2 The PVs under strong light

During the time between 12 am to 14 pm, the light of the sun is strong. Thus the power output of the PVs is high and it is 0.9 pu. Under this case, a three phase fault to ground occurs at the midpoint of the transmission line 2~3 at 0.5 s, and then it is cleared by the relay protection after 0.1 s. The virtual inertia of the PV-VSG under the variable inertia control strategy is shown in Fig. 8. It could be found that the VSG's virtual moment of inertia is controlled by the proposed bang-bang control strategy. When the angular speed difference between the SG and the PV-VSG $\omega_{AB} > 0$, namely the SG's angular speed is faster than the VSG's virtual angular speed, the virtual inertia of the PV-VSG J_{vsg} turns to the maximum values and it equals to 35 pu. When the SG's angular speed is lower than the PV-VSG's virtual angular speed, namely $\omega_{AB} < 0$, the virtual inertia of the PV-VSG turns to a small value $J_{vsg} = 5$ pu. Otherwise, if the

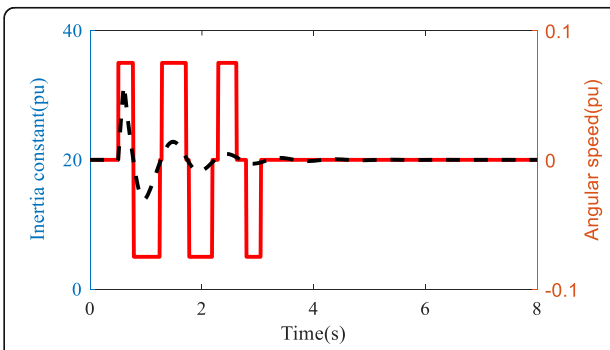

Fig. 8 The Virtual inertia of the PV-VSG and the angular speed difference under the variable inertia strategy

angular speed difference between the SG and the PV-VSG satisfies the following relation $|\omega_{AB}| < 0.001$pu, the virtual inertia of the PV-VSG $J_{vsg} = 20$pu. Under the constant inertia control strategy, the virtual inertia of the PV-VSG is fixed. It equals to the average value under the variable inertia case $J_{vsg} = 20$pu.

For comparative analysis, the angular speed difference between the SG and the PV-VSG under the three control strategies is shown in Fig. 9. It could be found that the angular speed will oscillate after the fault. If the PVs is operated under the MPPT mode and no PV-VSG control strategy is applied, the oscillation is hard to decay. When the PV-VSG control strategy with constant inertia is adopted, the oscillation will be suppressed quickly. What is more, the oscillation after fault will recover to a stable state faster when the variable inertia control strategy is applied.

Under the three control strategies, the active power output of the SG and the PV-VSG are shown in Figs. 10 and 11. From the simulation results, it is obvious to get that the active power output of both SG and VSG would take less time to return to a stable state under the variable inertia control strategy. It means that the unbalanced transient energy would be suppressed more quickly and the system is more easily to keep stability by the variable inertia control of the PV-VSG. Therefore, it is verified that the bang-bang control strategy of VSG's inertia could effectively dissipate the unbalanced energy of power system after the disturbance.

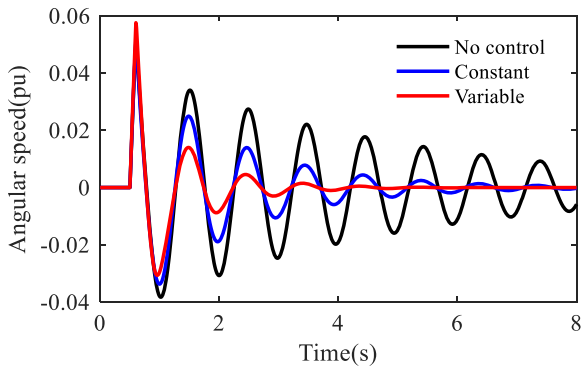

Fig. 9 The angular speed difference between the SG and the PV-VSG when the output power of the PV is 0.9 pu

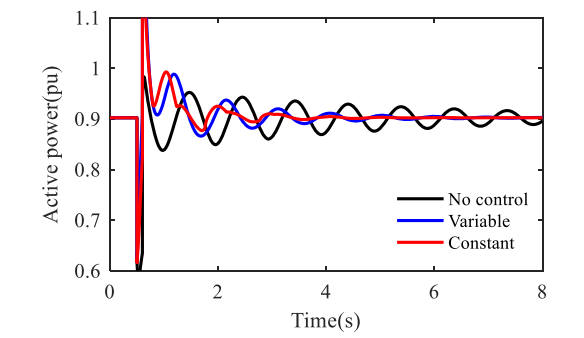

Fig. 10 The active power output of the PV-VSG when the output power of the PV is 0.9 pu

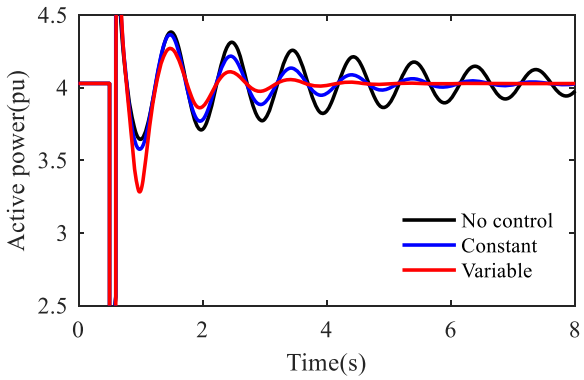

Fig. 11 The active power output of the SG when the output power of the PV is 0.9 pu

The power output of the ESS under the PV-VSG control strategies are shown in Fig. 12. From Fig. 12, it could be observed that, under the variable inertia control strategy, the ESS provides more energy support in the first and second swings of power oscillation. Then the power system achieves a faster dissipation of unbalanced power. It takes less time for the ESS to stable the power system under the variable inertia control.

4.3 The PVs under weak light

When the light of the sun is weak, the power output of the PVs will decrease to 0.09pu. In such situation, the power output of the SG increases to 4.84pu. When the same fault occurs at the midpoint of the transmission line 2~3, the simulation results are

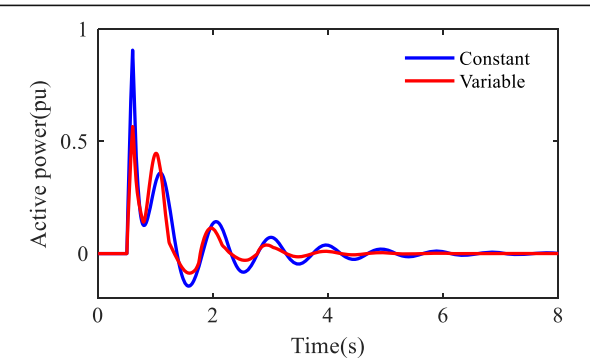

Fig. 12 The Active power output of ESS when the output power of the PV is 0.9 pu

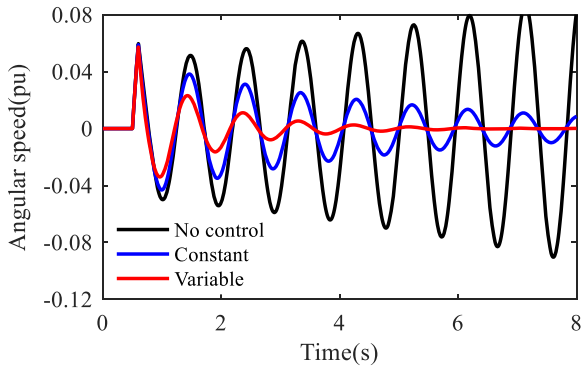

Fig. 13 The angular speed difference between the SG and the PV-VSG when the output power of the PV is 0.09 pu

shown in Figs. 13, 14, 15, 16 and 17. From the simulation results, it is found that the damping ratio of the PV power system turns to negative after the fault if no PV-VSG control strategy is applied. The angular speed difference between the SG and the PV-VSG oscillate with increasing oscillation amplitude.

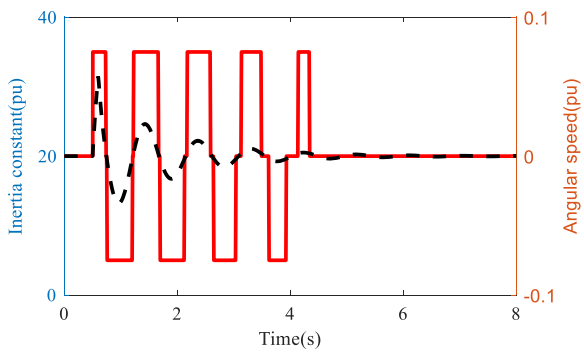

Fig. 14 The Virtual inertia of the PV-VSG when the output power of the PV is 0.09 pu

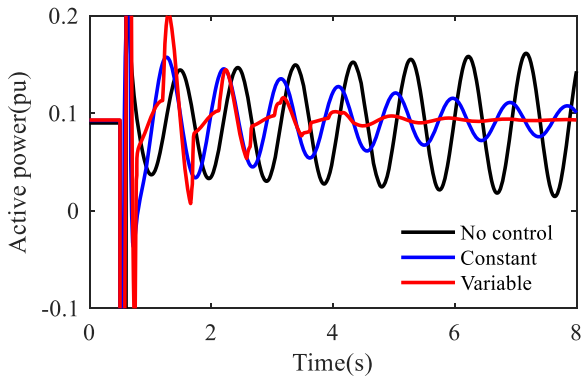

Fig. 15 The active power output of the PV-VSG when the output power of the PV is 0.09 pu

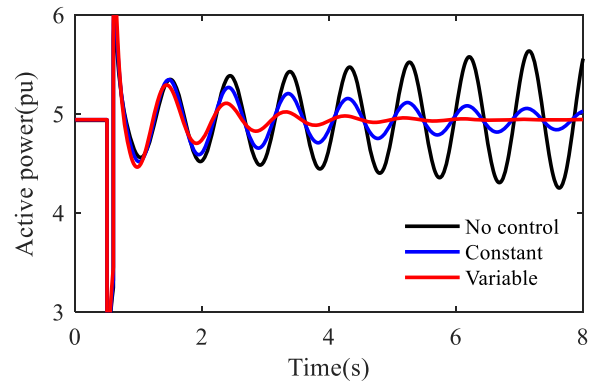

Fig. 16 The active power output of the SG when the output power of the PV is 0.09 pu

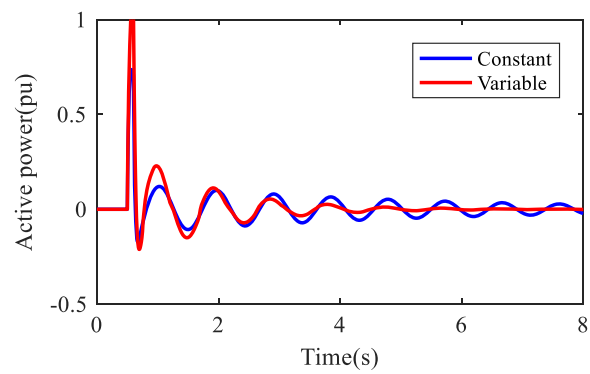

Fig. 17 The Active power output of ESS when the output power of the PV is 0.09 pu

Also, the oscillations of the power output of the SG and PVs are followed. Then the PV power system will lose stability.

When the PV-VSG control strategy with constant inertia is utilized, the oscillation of the PV power system will slowly decay after the fault. The PV power system will recover to a stable state after more than ten oscillation cycles. The PV power system will be able to keep stable under the same fault. It indicates that the PV-VSG control strategy could improve the stability of the PV power system.

If the PV-VSG control strategy with variable inertia proposed in this paper is adopted, the ESS wills response to the disturbance after the fault. The virtual inertia of the PV-VSG is shown in Fig. 14. When the angular speed difference between the SG and the PV-VSG is larger than zero, the virtual inertia of the PV-VSG increases to 35 pu. Compared with that of the constant inertia case, the power output of the ESS will decrease. Then less unbalance transient

energy will be injected into the PV power system. When the angular speed difference between the SG and the PV-VSG is less than zero, the inertia of the PV-VSG decreases to 5 pu. Then the power output of the ESS will be increased to suppress the unbalance transient energy. Under such a control strategy, the transient energy of the PV power system will decay quickly. The PV power system will recover to the stable state fast after the fault. The PV-VSG control strategy with variable inertia could further improve the stability of the PV power system.

5 Discussion

The PV-VSG control could help the PV power system keep stable after the fault. Especially, the variable inertia control strategy based on transient energy could help the PV power system suppress the transient energy. Thus the oscillation after the fault will decay quickly, which is beneficial for the PV power system to keep stable.

6 Conclusions

The VSG control strategy has been introduced to improve the power output characteristic of the renewable energy. Considering the adjustability of VSG's virtual moment of inertia, we proposed a bang-bang control strategy for the VSG's virtual inertia based on the TEF decay method. When the PV-VSG is on the receiving side, and the difference of the angular speed between the sending side and receiving side is positive, the inertia of the PV-VSG is set to a larger value, otherwise, it is set to a smaller value. Under this control strategy, the TEF of the power system after disturbance will decay quickly, and the transient stability of the power system with high penetration PVs will be improved.

Authors' contributions

Dr. LJ proposes the control strategy of the virtual synchronous generators (VSG); Dr. YDJ and Dr. YW offer the ideal of alternating inertia of VSG; Dr. ZHS, Dr. FRC and Dr. WB help to collect the data for simulation and achieve the simulation in MATLAB. All authors read and approved the final manuscript.

Competing interests

The authors declare that they have no competing interests.

Author details

[1]State Grid Hubei Economic Research Institute, Wuhan, China. [2]State Key Laboratory of Advanced Electromagnetic Engineering and Technology, and School of Electrical and Electronic Engineering, Huazhong University of Science and Technology, Wuhan, China.

Received: 20 June 2017 Accepted: 13 October 2017
Published online: 22 November 2017

References

1. Kundur, P. (1993). *Power System Stability and Control*. New York: McGraw-Hill.
2. Fang, D. Z., Xiaodong, Y., Wennan, S., & Wang, H. F. (2003). Oscillation transient energy function applied to the design of a TCSC fuzzy logic damping controller to suppress power system interarea mode oscillations. *IEE Generation Transm Distrib, 150*(2), 233–238.
3. Alipoor, J., Miura, Y., & Ise, T. (2015). Power system stabilization using virtual synchronous generator with variable moment of inertia. *IEEE J Emerg Sel Topic Power Electron, 3*(2), 451–458.
4. Khayyer, P., & Özgüner, U. (2014). Decentralized control of large-scale storage based renewable energy systems. *IEEE Trans Smart Grid, 5*(3), 1300–1307.
5. Sui, X., Tang, Y., He, H., & Wen, J. (2014). Energy-storage-based low frequency oscillation damping control using particle swarm optimization and heuristic dynamic programming. *IEEE Trans Power Syst, 29*(5), 2539–2548.
6. Gong, Y., Jiang, Q., & Baldick, R. (2016). Ramp event forecast based wind power ramp control with energy storage system. *IEEE Trans Power Syst, 31*(3), 1831–1844.
7. van Wesenbeeck M. P. N., de Haan S. W. H., Varela P., K. Visscher. Grid tied converter with virtual kinetic storage. in *Proc. IEEE Bucharest PowerTech*, Bucharest; 2009, pp. 1–7.
8. Torres M., Lopes L. A. C. Virtual synchronous generator control in autonomous wind-diesel power systems, in *Proc. IEEE Elect. Power Energy Conf. (EPEC)*, Montreal; 2009, pp. 1–6.
9. V. Karapanos, S. de Haan, and K. Zwetsloot, "Real time simulation of a power system with VSG hardware in the loop," in Proc. 37th Annu. Conf. IEEE Ind. Electron. Soc. (IECON), Nov. 2011, pp. 3748–3754.
10. Liu, J., Miura, Y. S., Bevrani, H., & Ise, T. Enhanced virtual synchronous generator control for parallel inverters in microgrids. *IEEE Trans Smart Grid*. doi:10.1109/TSG. 2016.2521405.
11. Li, C. Y., Xu, J. Z., & Zhao, C. Y. (2016). A coherency-based equivalence method for MMC inverters using virtual synchronous generator control. *IEEE Trans Power Delivery, 31*(3), 1369–1378.
12. Shintai, T., Miura, Y., & Ise, T. (2014). Oscillation damping of a distributed generator using a virtual synchronous generator. *IEEE Trans Power Delivery, 29*(2), 668–676.
13. Hirase, Y., Sugimoto, K., Sakimoto, K., & Ise, T. (2016). Analysis of resonance in microgrids and effects of system frequency stabilization using a virtual synchronous generator. *IEEE J. Emerg Sel Top Power Electronic, 4*(4), 1287–1298.
14. Zhao, H. L., Yang, Q., & Zeng, H. M. (2017). Multi-loop virtual synchronous generator control of inverter-based DGs under microgrid dynamics. *IET Generation Transm Distrib, 11*(3), 795–803.
15. Lu, L. Y., & Chu, C. C. (2015). Consensus-based secondary frequency and voltage droop control of virtual synchronous generators for isolated AC micro-grids. *IEEE J Emerg Sel Top Circuits Syst, 5*(3), 443–455.
16. Liu, J., Wen, J., Yao, W., & Long, Y. (2016). Solution to short-term frequency response of wind farms by using energy storage systems. *IET Renewable Power Generation, 10*(5), 669–678.
17. Ma, Y. W., Cao, W. C., Liu, Y., Wang, F., & Tolbert, L. M. Virtual synchronous generator control of full converter wind turbines with short term energy storage. *IEEE Trans Ind Electron*. doi:10.1109/TIE.2017.2694347.
18. Ortega, and F. Milano. Generalized model of VSG-based energy storage systems for transient stability analysis. *IEEE Trans Power System*. 2015. doi:10.1109/TPWRS.2015.2496217.